Basic Research in Cardiology (2019) 114:12
https://doi.org/10.1007/s00395-019-0721-6

ORIGINAL CONTRIBUTION

# The different response of cardiomyocytes and cardiac fibroblasts to mitochondria inhibition and the underlying role of STAT3

Jing Zhao[1,2] · Jin-Lai Gao[1,2] · Jun-Xue Zhu[1,2] · Hai-Bin Zhu[1,2] · Xuan Peng[1,2] · Man Jiang[1,2] · Yao Fu[1,2] · Juan Xu[1,2] · Xi-Hai Mao[1,2] · Nan Hu[1,2] · Ming-Hui Ma[1,2] · De-Li Dong[1,2]

Received: 27 November 2018 / Accepted: 12 February 2019 / Published online: 14 February 2019


## Abstract

Cardiomyocyte loss and cardiac fibrosis are the main characteristics of cardiac ischemia and heart failure, and mitochondrial function of cardiomyocytes is impaired in cardiac ischemia and heart failure, so the aim of this study is to identify fate variability of cardiomyocytes and cardiac fibroblasts with mitochondria inhibition and explore the underlying mechanism. The mitochondrial respiratory function was measured by using Oxygraph-2k high-resolution respirometry. The STAT3 expression and activity were evaluated by western blot. Cardiomyocytes and cardiac fibroblasts displayed different morphology. The mitochondrial respiratory function and the expressions of mitochondrial complex I, II, III, IV, and V of cardiac fibroblasts were lower than that of cardiomyocytes. Mitochondrial respiratory complex I inhibitor rotenone and $H_2O_2$ (100 μM, 4 h) treatment induced cell death of cardiomyocyte but not cardiac fibroblasts. The function of complex I/II was impaired in cardiomycytes but not cardiac fibroblasts stimulated with $H_2O_2$ (100 μM, 4 h) and in ischemic heart of mice. Rotenone and $H_2O_2$ (100 μM, 4 h) treatment reduced STAT3 expression and activity in cardiomyocytes but not cardiac fibroblasts. Inhibition of STAT3 impaired mitochondrial respiratory capacity and exacerbated $H_2O_2$-induced cell injury in cardiomycytes but not significantly in cardiac fibroblasts. In conclusion, the different susceptibility of cardiomyocytes and cardiac fibroblasts to mitochondria inhibition determines the cell fate under the same pathological stimuli and in which STAT3 plays a critical role.

**Keywords** Cardiomyocytes · Cardiac fibroblasts · STAT3 · Mitochondria · $H_2O_2$

## Introduction

Cardiomyocyte loss and the subsequent cardiac fibrosis are the general characteristics of severe heart diseases such as cardiac ischemia and heart failure [29, 34]. Cardiomyocytes and cardiac fibroblasts are the dominant cell types in the heart. Although both cardiomyocytes and cardiac fibroblasts suffer the same pathological stimuli like ischemia simultaneously when ischemia occurs, cardiomyocytes are lost through apoptosis or necrosis but cardiac fibroblasts begin to proliferate and transform from fibroblasts to myofibroblasts, thereby increasing the extracellular matrix of collagen deposition and triggering interstitial fibrosis [21]. Thus, a basic question arises, why cardiomyocytes and cardiac fibroblasts show contrary phenotype under the same pathological stimuli.

Mitochondria are the crucial organelles sensing oxygen supply and providing efficient energy for cardiomyocyte contraction [4]. Mitochondrial function of cardiomyocytes is inhibited in various heart diseases, for instance,

**Electronic supplementary material** The online version of this article (https://doi.org/10.1007/s00395-019-0721-6) contains supplementary material, which is available to authorized users.

Jing Zhao and Jin-Lai Gao contributed equally to the work.

✉ De-Li Dong
dongdeli@ems.hrbmu.edu.cn

[1] Department of Pharmacology (the State-Province Key Laboratories of Biomedicine-Pharmaceutics of China, Key Laboratory of Cardiovascular Research, Ministry of Education), College of Pharmacy, Harbin Medical University, Baojian Road 157, Harbin 150086, People's Republic of China

[2] Translational Medicine Research and Cooperation Center of Northern China, Heilongjiang Academy of Medical Sciences, Harbin Medical University, Harbin, People's Republic of China

the mitochondrial complex I activity was impaired during cardiac ischemia and heart failure [38, 42]. The impaired mitochondria triggered cardiomyocyte apoptosis and necrosis through the intrinsic mitochondrial pathway or opening of the mitochondrial permeability transition pore [12, 28]. However, cardiac fibroblasts also possess mitochondria; under such circumstances, the change of mitochondrial function of cardiac fibroblasts and the potential role of mitochondria of cardiac fibroblasts in these heart diseases are still unclear. As for the question put forward above, we speculate that the response of cardiomyocytes and cardiac fibroblasts to mitochondrial impairment is different and the difference determines the contrary phenotypes of cardiomyocytes and cardiac fibroblasts under the same pathological stimuli. If so, the potential molecular mechanisms need to be further elucidated.

Signal transducer and activator of transcription 3 (STAT3) plays a protective role against cardiomyocyte injury [1, 11, 14, 16, 30]. Nevertheless, STAT3 promotes cardiac fibroblast proliferation, fibrosis-related gene expression, and conversion to myofibroblast to induce fibrosis [17, 36]. STAT3 is associated with mitochondrial function. On the one hand, STAT3 activation enhances mitochondrial function of cardiomyocytes [3]; on the other hand, our previous study finds that inhibition of mitochondrial function significantly represses STAT3 activity in cardiomyocytes [10]. Collectively, we speculate that STAT3 might be the key factor determining the different response of cardiomyocytes and cardiac fibroblasts to the same pathological stimuli.

Based on the above analysis, we design the project to investigate the different response of cardiomyocytes and cardiac fibroblasts to mitochondria inhibition and explore the underlying molecular mechanisms.

## Methods

### Reagents

Digitonin, glutamate, malate, ADP, succinate, oligomycin, FCCP, rotenone and antimycin A were provided by Sigma-Aldrich (USA). Hydrogen peroxide ($H_2O_2$) was purchased from Melone Pharmaceutical Co., Ltd (Dalian, China). Mitotracker and DAPI were purchased from Life technology (Invitrogen, Oregon, USA). STAT3 inhibitor S3I-201 was purchased from EMD Millipore (Billerica, MA USA). Antibody against p-STAT3(Y705), p-STAT3(S727), STAT3, p-JAK2, JAK2, p-Akt(S473), p-Akt(T308), Akt, p-GSK-3β(Ser9), GSK-3β, VDAC and COXIV antibodies were bought from Cell Signaling Technology (Danvers, MA, USA). Total OXPHOS rodent WB antibody cocktail was purchased from Abcam (Cambridge, MA, USA). Anti-SDHA and anti-SDHB antibodies were purchased from Biosynthesis Biotechnology (Beijing, China), and anti-SDHC antibody was from Santa Cruz Biotechnology (Dallas, TX, USA). Anti-actin antibody and anti-GAPDH antibody were provided by ZSGB-BIO (Beijing, China).

### Isolating and culturing neonatal rat primary cardiomyocytes and cardiac fibroblasts

The primary cardiomyocytes and cardiac fibroblasts from neonatal Sprague–Dawley rats for 1–2 days were cultured by a conventional method used in our and other studies [10, 23, 32, 37]. Briefly, the hearts were removed from the animals and cut into 1-$mm^3$ pieces. After that, the chunks were digested by 0.25% trypsin. Then, cells were suspended in Dulbecco's modified Eagle's medium/medium (DMEM) with 10% fetal bovine serum, 100 U/ml penicillin and 100 μg/ml streptomycin. The resuspension was plated onto a culture flask for 90 min in humidified incubator (95% air–5% $CO_2$) to obtain cardiac fibroblasts for their selective adhesion. Then, the suspended cardiomyocytes were transferred and seeded into another plates. 5-Bromo-2-deoxyuridine (5-BrdU, 10 nM; #B5002; Sigma, Saint Louis, USA) was added to the cardiomyocytes to prevent proliferation of non-cardiomyocytes. Cardiac fibroblasts (passages 2–3) were grown to subconfluence in serum-containing media. Forty-eight hours later, cardiomyocytes and cardiac fibroblasts were employed for subsequent experimental procedures, respectively. The purity of cultured cardiomyocytes and cardiac fibroblasts satisfied the experiment requirements as identified by the cardiomyocyte and cardiac fibroblast-specific marker staining (Supplementary Fig. 1).

### Mouse myocardial ischemia (MI) model

Kunming mice (22–25 g weight, male) were used for animal studies and kept at standard laboratory conditions of temperature and humidity with a 12-h light/dark cycle. All experiments were performed according to the National Institutes of Health guide for the care and use of Laboratory animals, and were treated ethically. The study was approved by the Ethic Committees of Harbin Medical University (No. HMUIRB20180012). The detailed procedures for establishing a mouse model of myocardial ischemia were described as in previously studies [5, 19, 26]. Briefly, mice were anesthetized with avertin (0.2 g/kg, ip; T48402; Sigma-Aldrich Corporation, St. Louis, MO, USA). After opening the chest to expose the heart, left anterior descending artery (LAD) was ligated with a 7/0 nylon suture at 2 mm below the border between left atrium and ventricle to establish MI. The mice in sham group were treated consistently with the same experimental procedures in the MI group but without ligation of LAD. And electrocardiogram (ECG) was recorded to validate ischemic status characterized by ST segment

significant elevation. After ischemia for 30 min, ischemic zone was collected, and samples at the same position in sham group were collected for mitochondrial respiration detection.

### Lactate dehydrogenase (LDH) release assay

The LDH release from cardiomyocytes and cardiac fibroblasts was determined using commercial kit (Beyotime Biotechnology, China). The OD value of LDH was recorded at the wavelength of 490 nm.

### Cell viability measurement

Cell viability was assessed using the MTT assay as described in our previous studies [43, 44]. Briefly, cells were seeded in 96-well flat-bottomed plates at $5 \times 10^3$ cells per well, treated with or without $H_2O_2$ and/or STAT3 inhibitor (S3I-201)/si-STAT3 and incubated with MTT (5 mg/mL) for 4 h at 37 °C, and 200 µl dimethyl sulfoxide (DMSO) was added to dissolve the insoluble purple formazan product. The absorbance was then measured at 490 nm using a plate reader (Tecan Infinite m200, Mannedorf, Switzerland).

### Live and dead cell staining

The live and dead cells were detected using the LIVE/DEAD® Viability/Cytotoxicity Assay Kit (Invitrogen, Waltham, MA, USA) as described in our previous studies [43, 44]. Briefly, cardiomyocytes and cardiac fibroblasts were, respectively, seeded into the six-well plate at $5 \times 10^4$ cells per well and incubated with a mixture of 2 µM calcein AM and 4 µM EthD-1 for 15 min at 37 °C. The labeled cells were randomly visualized on a fluorescence microscope (Olympus IX73 with DP73 camera, Japan) at 20× magnification and counted using ImagePro Plus image analysis software (Media Cybernetics Inc, Silver Spring).

### Mitochondrial respiratory function detection

Mitochondrial respiratory function was examined in heart tissues, cardiomyocytes and cardiac fibroblasts. First, approximately 4 mg heart tissue was cut and ground in PBS buffer, and then centrifuged at 3500 rpm for 5 min. After that, the tissue precipitation with the mitochondrial respiration solution (MiR05) was resuspended for the following mitochondrial respiratory function detection. The MiRO5 consisted of EGTA 0.5 mM, $MgCl_2 \cdot 6\ H_2O$ 3 mM, Lactobionic acid 60 mM, Taurine 20 mM, $KH_2PO_4$ 10 mM, HEPES 20 mM, D-sucrose 110 mM, BSA, and essentially fatty acid free 1 g/l.

Second, after pretreatment, cardiomyocytes and cardiac fibroblasts were harvested via trypsin digestion and centrifuged at 800 rpm for 5 min at room temperature. Then, the pellet was resuspended in cell culture medium or MiR05 for high-resolution respirometry. Mitochondrial respiratory function was measured in a two-chamber titration injection respirometer (Oxygraph-2k; Oroboros Instruments, Innsbruck, Austria). The final density of cell suspension in the detected chamber was approximately $1 \times 10^6$ cells/ml. After stabilization for 5 min, close the chamber and make calibration for $O_2$ concentration in the chamber. Data were recorded through DatLab software 5.2 (Oroboros Instruments, Innsbruck, Austria).

To detect mitochondrial respiratory function of cardiomyocytes and fibroblasts, two classical protocols were adopted, respectively, in intact cells with phosphorylation control protocol and specifically in permeabilized cells with substrate–uncoupler–inhibitor titration protocol [7, 45]. In detail, the intact cell measure protocols were as following: routine respiration (Routine) was followed by manual titration of oligomycin (Omy, 2 µg/ml) to induce the non-phosphorylating leak state and uncoupler (1 mM FCCP) in steps of 2 µl corresponding to a step increase in the final concentration of 1 µM FCCP at intervals of 120 s till maximum noncoupled flux (capacity of the electron transfer system, ETS) was induced. Maximal mitochondrial respiration (MMR) in mitochondria of cardiomyocytes and cardiac fibroblasts was calculated by subtract the oxygen consumption rate (OCR) elicited by oligomycin from maximum oxygen consumption rate induced by FCCP. Reserve respiratory capacity (RRC) was equal to the difference between maximum oxygen consumption rate and routine oxygen consumption rate.

In permeabilized cells, we used the protocol with substrate–uncoupler–inhibitor titrations. After respiration was stabilized for a short time, routine respiration was measured. Then, digitonin (Dig, 150 µg/$10^6$ cells) was applied for plasma membrane permeabilized. Glutamate (G, 5 mM) and malate (M, 2 mM) in the absence of ADP titration were used for inducing the respiratory leak state of complex I ($CI_{Leak}$). Then, 5 mM ADP added was to detect the oxidative phosphorylation (OXPHOS) capacity of complex I (CIP). Maximal OXPHOS capacity was induced by succinate (100 mM), including both CI and complex II OXPHOS capacity (CII, CI + IIP). Next, oligomycin and FCCP titrations were used for the maximal uncoupled respiratory capacity of the electron transfer system (ETS) (CI + IIETS). CII-related uncoupled respiratory function (CIIETS) was detected after the addition of rotenone (Rot, 0.5 µM). Finally, antimycin A (Ama, 2.5 µM) was given for residual oxygen consumption evaluation.

### Western blot

Total protein was extracted and separated from both cardiomyocytes and cardiac fibroblasts for immunoblotting analysis with the procedures described in our previous work [24]. Membranes were incubated with primary antibodies against p-STAT3 Y705 (1:500), p-STAT3 S727 (1:500), STAT3 (1:500), p-Akt S473 (1:500), p-Akt T308 (1:500), Akt (1:500), p-JAK2 (1:500), JAK2 (1:500), p-GSK-3β Ser9 (1:500), GSK-3β (1:500), VDAC (1:500), COXIV (1:500), SDHA (1:250), SDHB (1:250), and SDHC (1:250), Total OXPHOS rodent WB antibody cocktail (1:250), β-Actin (1:1000) or GAPDH (1:1000) overnight at 4 °C, and then incubated with a fluorescence-labelled secondary antibody (LI-COR Biosciences, Lincoln, NE, USA). The images were scanned by the Odyssey CLx Infrared Imaging System (LI-COR Biosciences). The bands were quantified with Odyssey CLx Image Studio 5.0 software and normalized to actin as an internal control.

### Mitochondrial staining

The mitochondrial morphology was observed using mitochondrial staining with MitoTracker® probes (Cell signaling technology, USA) as described in our previous work [24]. Briefly, cultured cardiomyocytes and cardiac fibroblasts were loaded with Mito-Tracker Green (50 nM) for 25 min and Hoechst (1 μg/ml) for 15 min at 37 °C. Then, cells were washed by cultured medium without FBS for three times and imaged using Olympus Fluoview FV10i Olympus Confocal microscope (Tokyo, Japan).

### 5′-Bromodeoxyuridine (BrdUrd) incorporation

Cell proliferation was evaluated by Brdu incorporation according to the methods provided by BrdU Cell Proliferation ELISA kit (Abcam, Cambridge, UK). Dynamic information about cell cycle progression can be obtained by labeling cells with 5′-bromodeoxyuridine (BrdUrd) which is incorporated into DNA in place of thymidine. The value of BrdU incorporation was read by microplate reader at the wavelength of 550 nm.

### SiRNA transfection

Either siRNA (Genechem) targeting rat STAT3 or scrambled siRNA as negative control was transfected into cardiomyocytes and fibroblasts according to the manufacturer's instructions (GenePharma, suzhou, China). Briefly, 10 nM siRNA in serum-free and antibiotics-free DMEM containing 5 μl of Lipofectamine 2000 (Invitrogen) were premixed and transfected into cells. The medium was changed 8 h later with culture medium supplemented with FBS (Gibco). After stable transfection for 48 h, cells were treated with other drugs for the subsequent testing. RNA oligo sequences were listed as follows: (5′–3′): negative control, sense-UUCUCC GAACGUGUCACGUTT, antisense-ACGUGACACGUU CGGAGAATT; STAT3, sense-GGUCUCG GAAAUU UAA CAUTT, antisense-AUGUUAAAUUUCCGAGACCTT.

### Statistical analysis

All data were presented as mean ± SEM. Statistical analysis of the results was performed with GraphPad Prism version 7.0 (GraphPad Software Inc., San Diego, CA, USA). Statistical significance of two groups was determined with Student's *t* test. For two more groups, one-way ANOVA or two-way ANOVA followed by Dunnett test or Tukey's test was used. For the data with control value of 1 and no SEM, the randomized block ANOVA (repeated measures ANOVA) was used as described in previous Ref. [22]. $P < 0.05$ was considered statistically significant.

## Results

### The different mitochondrial morphology and function of cardiomyocytes and cardiac fibroblasts

Cardiomyocytes have a great demand of energy to perform contractile function and electrical activity. In contrast, cardiac fibroblasts are mainly responsible for synthesis and degradation of extracellular matrix and have low energy consumption. Due to the different energy demand, we suppose that the mitochondrial morphology and function would be distinct between the two types of cells. Thus, we cultured the rat primary neonatal cardiomyocytes and cardiac fibroblasts to observe their mitochondrial morphology first. The cardiomyocytes and cardiac fibroblasts could be easily differentiated under light microscope; cardiomyocytes had obvious refractivity and spontaneous beating while cardiac fibroblasts were in flat shape and no beating (Fig. 1a). We further stained the mitochondria of both types of cells with mito-Tracker. As shown in Fig. 1b, the mitochondria were abundant and most of the mitochondria were in rod shape in cardiomyocytes; whereas in cardiac fibroblasts, the amount of mitochondria was significantly less than that in cardiomyocytes and the mitochondria were in filamentous shape. Next, we compared the mitochondrial respiratory function of cardiomyocytes and cardiac fibroblasts using Oxygraph-2k high-resolution respirometry. The oxygen consumption was measured in intact cells with phosphorylation control protocol. Both the routine oxygen consumption and maximum oxygen consumption were lower in fibroblasts than those in cardiomyocytes (Fig. 1c, d). In addition, the function of

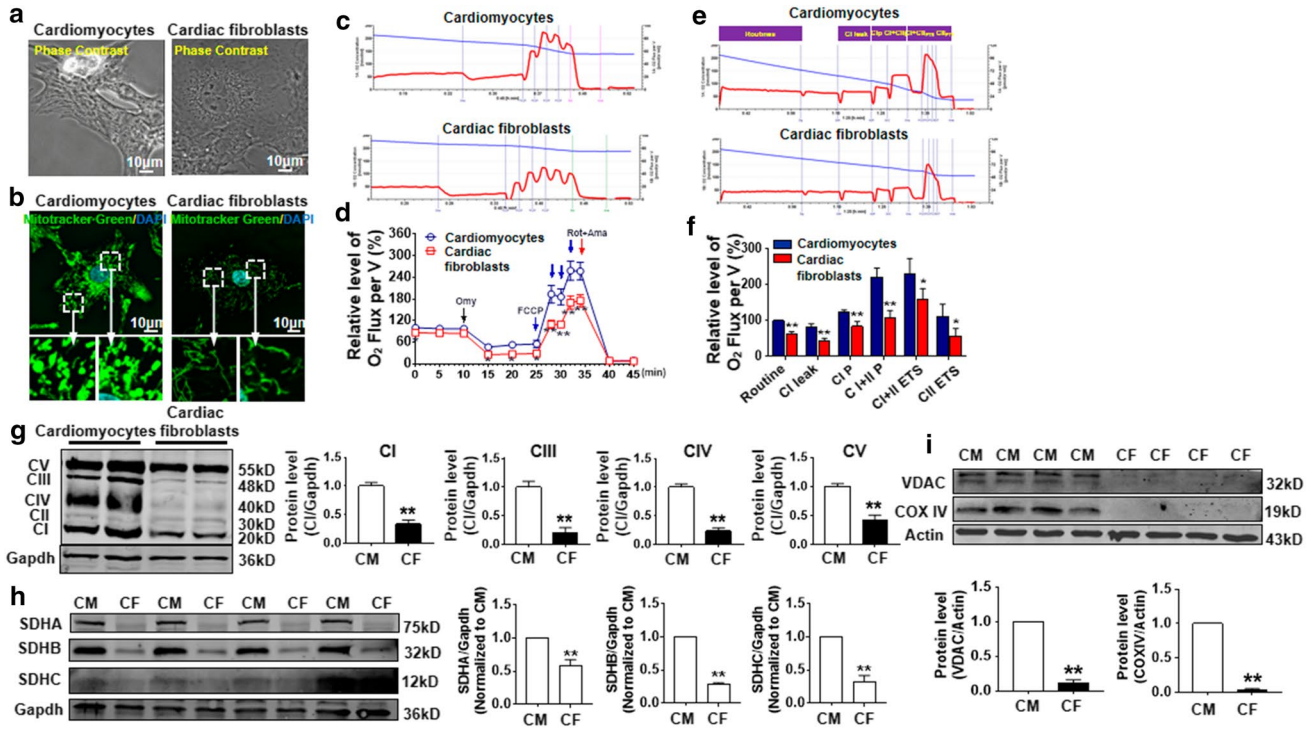


**Fig. 1** The mitochondrial morphology and respiration function of cardiomyocytes and cardiac fibroblasts. **a** The light microscopy images of primary cultured cardiomyocytes and cardiac fibroblasts. **b** The mitochondrial morphology of cardiomyocytes and cardiac fibroblasts stained with nucleus dye DAPI and mitochondria specific dye mitoTracker staining. **c** The mitochondrial respiratory function of cardiomyocytes and cardiac fibroblasts measured using Oxygraph-2k high-resolution respirometry. The oxygen concentration and oxygen flux of cardiomyocytes and cardiac fibroblasts in intact cells with phosphorylation control protocol in real time were determined. Oligomycin (Omy, 1 μM), FCCP (1, 2, 3, 4 μM), and rotenone (Rot, 1 μM) combined with antimycin A (Ama 1 μM) were added sequentially to cardiomyocytes or cardiac fibroblasts. Blue line stands for decreasing oxygen concentration in the oxygraphy chamber containing living cells. Red line stands for the changes of oxygen flux per volume. **d** The comparison of relative level of oxygen flux between cardiomyocytes and cardiac fibroblasts. $*P<0.05$, $**P<0.01$ vs cardiomyocyte, $n=6$ in each group. **e** Representative profiles of oxygen consumption of cardiomyocytes and cardiac fibroblasts in permeabilized cells with substrate–uncoupler–inhibitor titration protocol. Digitonin (Dig, 150 μg/$10^6$ cells), glutamate (G, 5 mM) and malate (M, 2 mM), ADP (5 mM), succinate (100 mM), Omy, FCCP, Rot and Ama were added sequentially to cardiomyocytes or cardiac fibroblasts. **f** The response of oxygen consumption of cardiomyocyte and cardiac fibroblast mitochondria to CI and II substrates. $*P<0.05$, $**P<0.01$ vs cardiomyocyte, $n=6$ in each group. **g** The protein expressions of mitochondrial respiratory complexes in cardiomyocytes and cardiac fibroblasts, including complex I, III, IV, and V. Left panel stands for the representative western blots and the right panels were the statistical data. $**P<0.01$ vs cardiomyocyte (CM). *CF* cardiac fibroblasts, $n=6$ for each group. **h** The expressions of succinate dehydrogenase subunits SDHA ($n=7$), SDHB ($n=7$), SDHC ($n=4$) in cardiomyocytes and cardiac fibroblasts. *CM* cardiomyocytes, *CF* cardiac fibroblats. $**P<0.01$ vs CM. **i** The protein expressions of mitochondrial marker protein VDAC ($n=8$) and COX IV ($n=8$) in cardiomyocytes and cardiac fibroblasts. Left panel stands for the representative western blots and the right panels were the statistical data. $**P<0.01$ vs cardiomyocyte (CM). *CF* cardiac fibroblasts, *VDAC* voltage-dependent anion channel. The protein level of VDAC and COX IV was normalized to that of actin

mitochondrial complex I/II was analyzed in permeabilized cells with coupling control protocol. Both the OXPHOS capacity and noncoupled state of electron transfer system capacity of complex I/II were lower in fibroblasts than those in cardiomyocytes (Fig. 1e, f). We compared the protein expression of mitochondrial complex I, II, III, IV, and V in cardiomyocytes and cardiac fibroblasts. Results showed that cardiac fibroblasts had a lower amount of respiratory chain components complex I, III, IV, and V than cardiomyocytes, but the complex II amount seemed to be comparable in fibroblasts and cardiomyocytes (Fig. 1g). In this experiment, the antibody mixture might had a low staining of the complex II components; to ensure the reliability of the results, we further measured the protein expressions of succinate dehydrogenase (SDH) subunits in cardiomyocytes and cardiac fibroblasts. As shown in Fig. 1h, the expressions of succinate dehydrogenase subunits SDHA, SDHB, SDHC in cardiac fibroblasts were significantly lower than that in cardiomyocytes.

We further examined the expressions of mitochondrial marker proteins VDAC (the voltage-dependent anion channel) and COX IV (cyclooxygenase-4) in cardiomyocytes and cardiac fibroblasts. Results showed that the level of actin in cardiomyocytes and cardiac fibroblasts was equivalent when

the same amount of cellular protein was used, but the levels of VDAC and COX IV normalized to actin in cardiac fibroblasts were significantly lower than that in cardiomyocytes (Fig. 1i). Together with the data of mitochondrial respiration function comparison (Fig. 1c–f), these results indicated that the amount of mitochondria of cardiac fibroblasts was less than that of cardiomyocytes. On the other hand, it seemed that the extent of difference in respiration between cardiomyocytes and fibroblasts was less than that in protein expressions of mitochondrial contents. This might be related to technical issues, as western blot signals in fibroblasts were below detection threshold.

## Effect of mitochondrial complex I inhibitor rotenone on cell survival of cardiomyocytes and cardiac fibroblasts

Since cardiomyocytes and cardiac fibroblasts have different mitochondrial morphology and function, we wonder the effect of mitochondrial complex inhibition on cell viability of the both types of cells. We treated cardiomyocytes and cardiac fibroblasts with complex I inhibitor rotenone at the same range of concentrations. As shown in Fig. 2a, rotenone treatment significantly increased the release of lactate dehydrogenase (LDH) from cardiomycytes; relatively, rotenone had no significant influence on LDH release from fibroblasts in the same dose range. To avoid the deviation induced by the different LDH content in cardiomyocytes and cardiac fibroblasts, we further used live/dead cell viability assays. The live/dead staining results further confirmed that rotenone induced more significant cell death in cardiomyocytes than in cardiac fibroblasts in the same dose range by using the two-way ANOVA analysis (Fig. 2b).

The cell proliferation of cardiac fibroblasts was detected after 12-h culture, and we further examined the effect of rotenone on the proliferative ability of cardiac fibroblasts using BrDU incorporation assay; rotenone ranged from 0.2 to 5 μM had no significant effect on cardiac fibroblast proliferation after 12-h culture (Supplementary Fig. 2a and 2b), indicating that inhibition of mitochondrial complex I activity showed no significant effect on cardiac fibroblast proliferation.

## $H_2O_2$ stimulus inhibits mitochondrial respiratory function and induces cell injury in cardiomyocytes but not in cardiac fibroblasts

$H_2O_2$ is an inducer of cell apoptosis and necrosis, and $H_2O_2$-induced cardiomyocyte injury generally mimics myocardial ischemia [25, 40]. $H_2O_2$-induced cell injury model was used. We treated the cultured cardiomyocytes and cardiac fibroblasts with $H_2O_2$ (100 μM) for 4 h and measured the mitochondrial function. We found that cardiomyocytes displayed a general reduction in respiration under $H_2O_2$

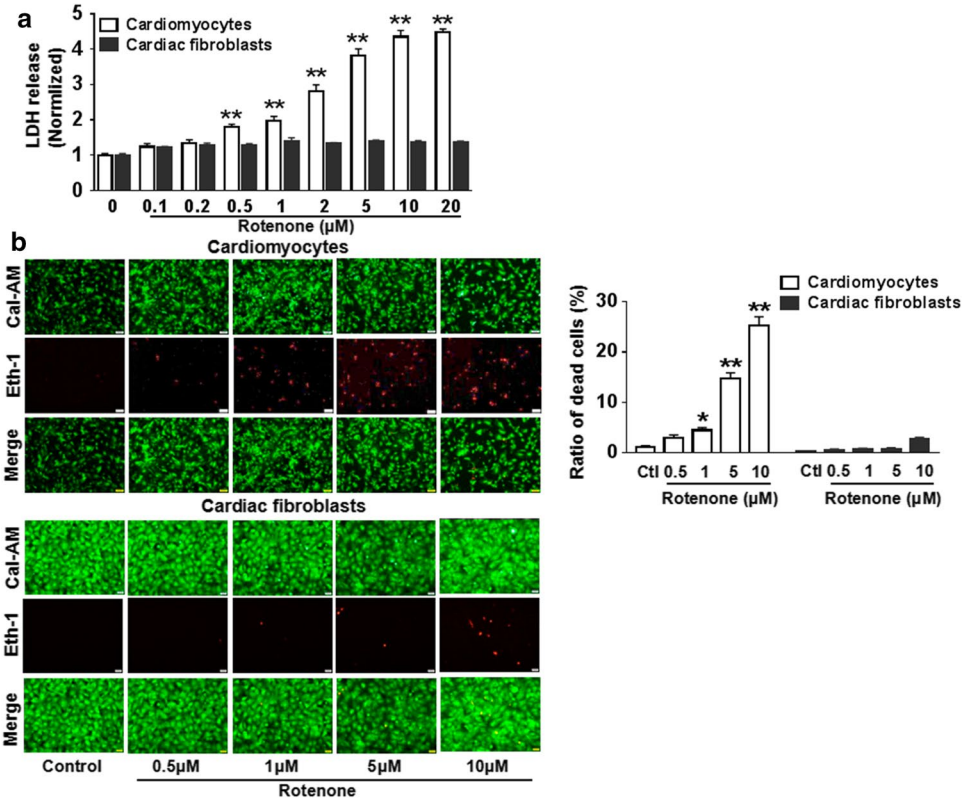


**Fig. 2** The cell survival of cardiomyocytes and cardiac fibroblasts treated with mitochondrial complex I inhibitor rotenone. **a** LDH release of cardiomyocytes and cardiac fibroblasts treated with rotenone (0.1–20 μM), $n=6$, $^{**}P<0.01$ vs cardiomyocyte treated with 0 μM rotenone. Two-way ANOVA followed by Tukey's test was used. **b** The images and statistical results of live/dead staining of cardiomyocytes and cardiac fibroblasts treated with rotenone. Two-way ANOVA followed by Tukey's test was used, $n=7$, $^{*}P<0.05$, $^{**}P<0.01$, vs control. *Ctl* control

stimulation (Fig. 3a, b). Specifically, all the cellular mitochondrial functional parameters, including routine respiration, maximum mitochondrial respiration (MMR) and residual respiration consumption (RRC), were markedly impaired in cardiomyocytes stimulated by $H_2O_2$ (100 μM) (Fig. 3c), which was consistent with previous reports [31]. However, the mitochondrial respiratory function of cardiac fibroblasts was unchanged under $H_2O_2$ (100 μM) stimulation, including routine respiration, MMR and RRC (Fig. 3d–f). We further examined the cell viability and LDH release of cardiomyocytes and cardiac fibroblasts stimulated with $H_2O_2$ ranged from 0 to 200 μM for 4 h. Results showed that, under the present experimental conditions, $H_2O_2$ induced significant cell death in cardiomyocytes but not cardiac fibroblasts (Fig. 3g, h); furthermore, $H_2O_2$ treatment did not affect the proliferation of cardiac fibroblasts, even increased the proliferation of cardiac fibroblasts at certain concentrations (5 μM and 10 μM) (Fig. 3i).

$H_2O_2$-induced cell injury depends on $H_2O_2$ concentrations and cell types. Our present experiment conditions differentiated the effect of $H_2O_2$ on cardiomyocytes and cardiac fibroblasts. However, when the time of $H_2O_2$ (100 μM) treatment was extended to 12 h or the concentration of $H_2O_2$ was increased to 500 μM (4 h), the cell death of cardiac fibroblasts was still induced (Supplementary Fig. 3).

## Impairment of complex I/II-related mitochondrial respiratory function in $H_2O_2$-stimulated cardiomyocytes and ischemic mice hearts

Since $H_2O_2$ stimulus inhibits mitochondrial respiratory function and induces cell injury in cardiomyocytes but not in cardiac fibroblasts, we further examined the mitochondrial respiration related to complex I and II in cardiomyocytes and cardiac fibroblasts. Mitochondrial respiration function represented with routine, CI leak, CI and CI plus CII oxidative phosphorylation (CIP and CI + IIP), as well as CI plus CII electron transfer system (CI + IIETS) and CIIETS was obviously decreased after exposure to $H_2O_2$ in cardiomyocytes (Fig. 4a, b), but no significant change was observed in cardiac fibroblasts (Fig. 4c, d). Then, we established cardiac ischemia model in mice by ligation of anterior descending coronary artery as described in other works [18–20]. After ischemia for 30 min, the ischemic zone was collected and the mitochondrial respiration function of myocardial tissues was measured. Compared with sham group, ischemic myocardial

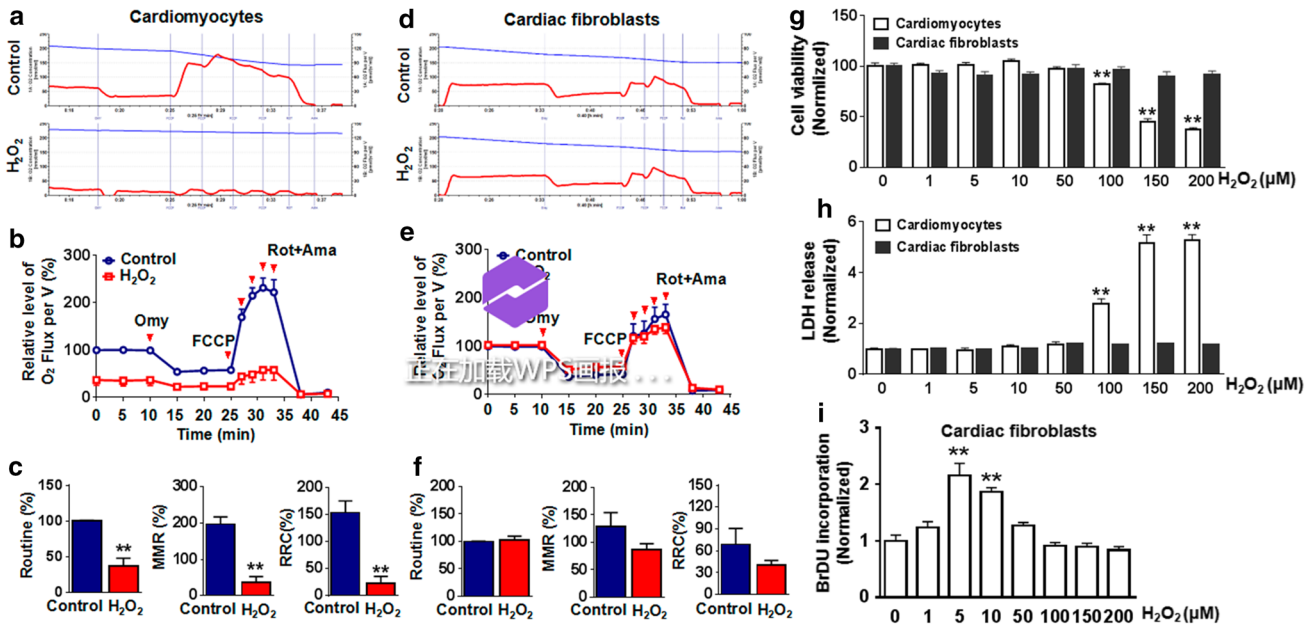


**Fig. 3** The mitochondrial respiratory function and cell survival of cardiomyocytes and cardiac fibroblasts treated with $H_2O_2$. **a**, **b** Representative profiles and statistical data of mitochondrial respiration of intact cardiomyocytes treated with $H_2O_2$ (100 μM, 4 h), $n = 8$. **c** $H_2O_2$ (100 μM, 4 h) treatment reduced routine respiration, maximum mitochondrial respiration (MMR) and residual respiration consumption (RRC) of cardiomyocytes, $n = 8$, $^{**}P < 0.01$, vs control. **d**, **e** Representative profiles and statistical data of mitochondrial respiration of intact cardiac fibroblasts treated with $H_2O_2$ (100 μM, 4 h), $n = 6$. **f** $H_2O_2$ (100 μM, 4 h) treatment showed no effect on routine respiration, maximum mitochondrial respiration (MMR) and residual respiration consumption (RRC) of cardiac fibroblasts, $n = 6$. **g** Effect of $H_2O_2$ (1–200 μM, 4 h) treatment on cell viability of cardiomyocytes and cardiac fibroblasts. $^{**}P < 0.01$, compared with 0 μM. Two-way ANOVA followed by Tukey's test was used, $n = 6$. **h** Effect of $H_2O_2$ (1–200 μM, 4 h) treatment on LDH release of cardiomyocytes and cardiac fibroblasts, $n = 6$, $^{**}P < 0.01$, compared with 0 μM. Two-way ANOVA followed by Tukey's test was used. **i** BrDU incorporation of cardiac fibroblasts treated with $H_2O_2$ from 1 to 200 μM, $n = 12$. $^{**}P < 0.01$ vs 0 μM

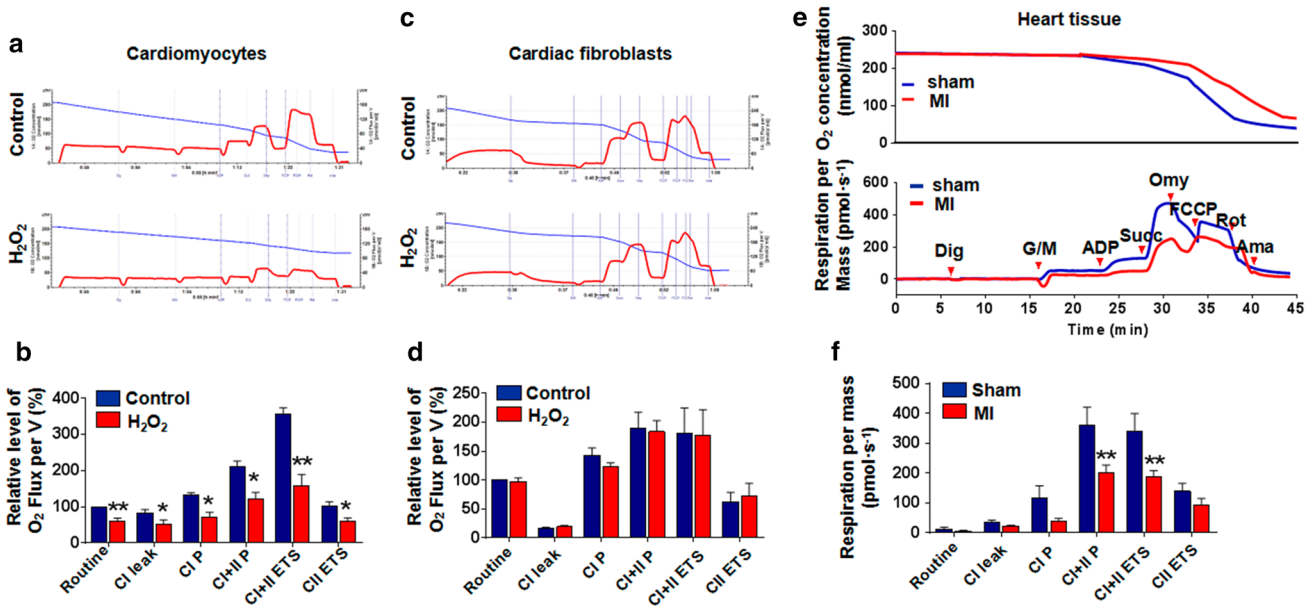


**Fig. 4** Mitochondrial respiratory function of cardiomyocytes and cardiac fibroblasts treated with $H_2O_2$ and mice heart after 30 min ischemia. **a**, **b** $H_2O_2$ (100 μM) treatment for 4 h inhibited mitochondrial complex of cardiomyocytes in permeabilized model. $^*P<0.05$, $^{**}P<0.01$ vs control, $n=6$. **c**, **d** $H_2O_2$ treatment for 4 h showed no effect on mitochondrial complex of cardiac fibroblasts in permeabilized model. **e** The representative profile of $O_2$ concentration change and relative level of $O_2$ flux per volume in sham and myocardial ischemia (MI) mice hearts. **f** The summarized data of mitochondrial respiration in sham and MI mice hearts, including routine, CI and CI plus CII oxidative phosphorylation, CI and CII leak, as well as CI plus CII electron transfer system. $^{**}P<0.01$ vs sham, $n=6$ for each group

tissues showed an overall reduction in mitochondrial function (Fig. 4e); furthermore, CI + IIP and CI + IIETS parameters were markedly reduced (Fig. 4f). These results indicated that the function of mitochondrial respiratory complex I/II in cardiomyocytes was mainly impaired in ischemic hearts.

## Mitochondrial complex I inhibitor rotenone and $H_2O_2$ inhibit STAT3 activity and expression in cardiomyocytes but not cardiac fibroblasts

The above data indicated that mitochondria inhibition induced cell injury of cardiomyocytes but not cardiac fibroblasts; we asked what was the molecular mechanism linking mitochondria inhibition with cell injury in cardiomyocytes. STAT3 is an important survival factor for cardiomyocytes and our previous study had found that STAT3 activity was sensitive to the change of mitochondrial function in cardiomyocytes [10], therefore, we examined the effect of mitochondrial complex I inhibitor rotenone on STAT3 expression and activity in cardiomyocytes and cardiac fibroblasts. As shown in Fig. 5a–d, rotenone treatment significantly repressed p-STAT3 (Y705), p-STAT3 (S727) and total STAT3 protein levels in cardiomyocytes but not cardiac fibroblasts. Akt is an established survival signal through phosphorylation of proapoptotic proteins in the heart. We further comparatively studied the effect of rotenone on Akt expression and activity in cardiomyocytes. Results showed that, at the concentrations inhibiting STAT3, rotenone treatment did not affect Akt and its downstream signal GSK3β expression and activities (Fig. 5e–h).

We further examined the effect of $H_2O_2$ (100 μM, 4 h) treatment on STAT3 activity and expression in cardiomyocytes and cardiac fibroblasts. Results showed that $H_2O_2$ (100 μM) treatment for 4 h reduced p-STAT3 (Y705), p-STAT3 (S727) and total STAT3 protein levels in cardiomyocytes but not cardiac fibroblasts (Fig. 6a–d), which was similar to the effect of rotenone (Fig. 5a–d). The $H_2O_2$-induced decrease of STAT3 phosphorylation might be due to the inhibition of STAT3 upstream signal JAK2 because that $H_2O_2$ treatment inhibited the JAK2 activity in cardiomyocytes (Fig. 6e, f).

STAT3-mediated cardioprotection is considered through two pathways, the canonical transcriptional action and the non-transcriptional regulation of electron transport chain. Although we did not focus on the STAT3 protein levels required to mediate gene expression, we further examined the effect of rotenone which inhibited STAT3 on STAT3-targeted gene bcl-2 expression in cardiomyocytes and cardiac fibroblasts; meanwhile, bax was also measured. Results showed that rotenone at 1 μM slightly reduced Bcl-2 protein level in cardiomyocytes but not in cardiac fibroblasts. Rotenone at 0.5 μM had reduced STAT3 activity, but showed no

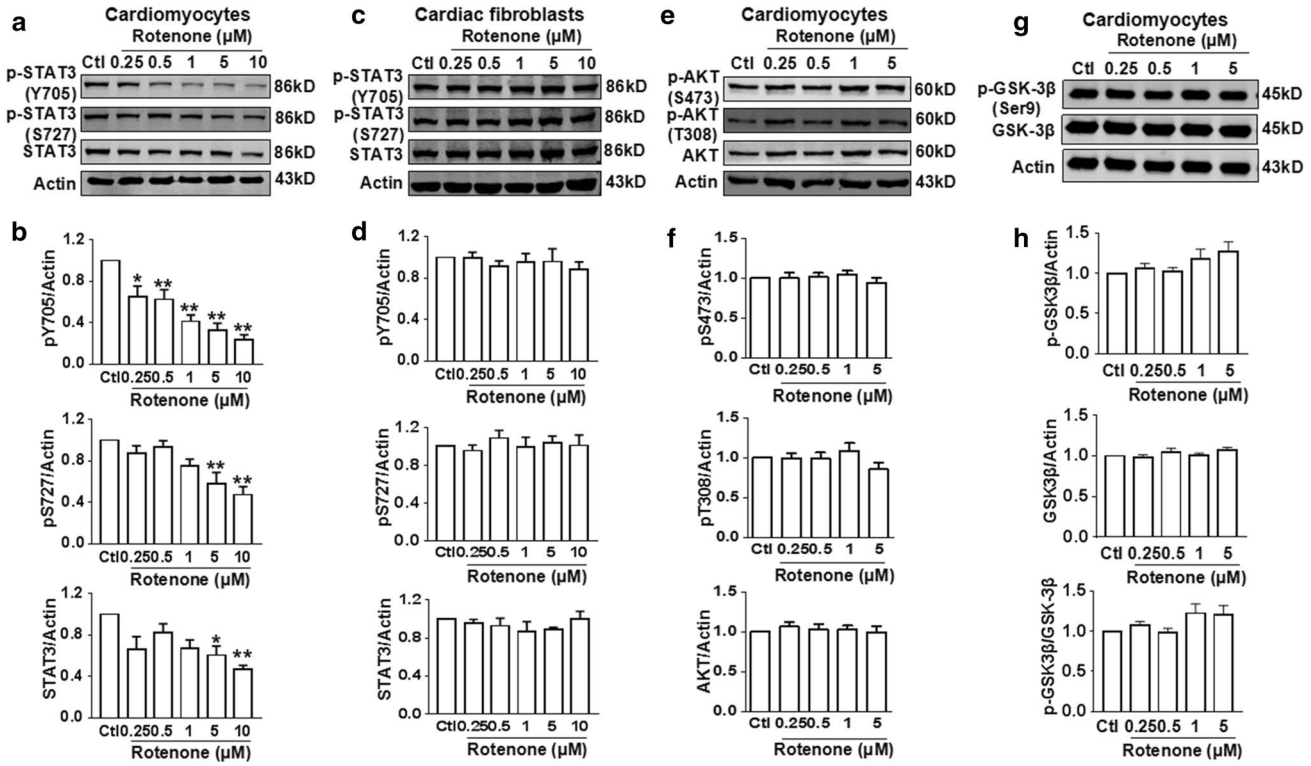


**Fig. 5** Mitochondrial complex I inhibitor rotenone inhibited STAT3 activity in cardiomyocytes but not cardiac fibroblasts. **a**, **b** Rotenone treatment for 12 h reduced STAT3 activity [reduced protein levels of pSTAT3 (Y705) and pSTAT3 (Y727)] and protein expression in cardiomyocytes, $n=6$, $^{*}P<0.05$, $^{**}P<0.01$ vs control. **c**, **d** Rotenone treatment for 12 h showed no effect on STAT3 activity and protein expression in cardiac fibroblasts, $n=6$. **e**, **f** Rotenone treatment for 12 h showed no effect on AKT activity and protein expression in cardiomycytes, $n=7$. **g**, **h** Rotenone treatment for 12 h showed no effect on GSK-3β activity and protein expression in cardiomycytes, $n=6$

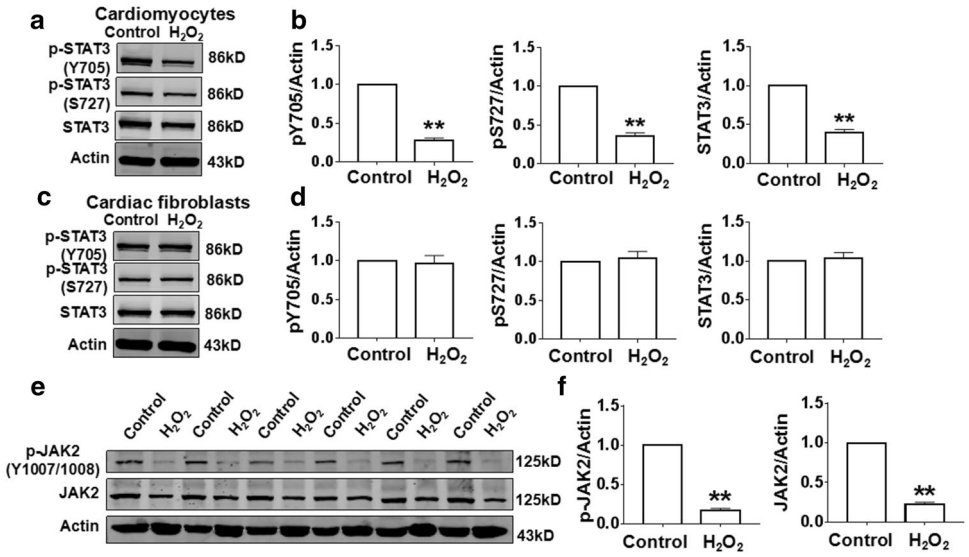


**Fig. 6** Effects of $H_2O_2$ on JAK2 and STAT3 expression in cardiomyocytes and cardiac fibroblasts. **a** Representative western blot bands of pSTAT3 (Y705), pSTAT3 (S727) and total STAT3 in control and $H_2O_2$ (100 μM, 4 h)-treated cardiomyocytes. **b** Statistical results of pSTAT3 (Y705), pSTAT3 (S727) and total STAT3.$^{**}P<0.01$ vs control, $n=6$. **c** Representative western blot bands of pSTAT3 (Y705), pSTAT3 (S727) and total STAT3 in control and $H_2O_2$ (100 μM, 4 h)-treated cardiac fibroblasts. **d** Statistical results of pSTAT3 (Y705), pSTAT3 (S727) and total STAT3, $n=6$. **e** Representative western blot bands of p-JAK2, JAK2 in control and H2O2 (100 μM, 4 h)-treated cardiomyocytes. **f** Statistical results of p-JAK2 and JAK2. $^{**}P<0.01$ vs control, $n=6$

effect on Bcl-2 expression in cardiomyocytes, indicating that the reduced STAT3 by mitochondrial inhibition in cardiomyocytes was not sufficient to influence target gene expression (Supplementary Fig. 4). Rotenone treatment showed no significant effect on bax protein level in cardiomyocytes and cardiac fibroblasts (Supplementary Fig. 4).

## Inhibition of STAT3 impairs complex I/II-related mitochondrial respiratory function and reduces cell viability in cardiomyocytes

Inhibition of mitochondrial function reduced STAT3 expression and activity in cardiomyocytes; conversely, we examined the effect of STAT3 inhibition on mitochondrial respiratory function and cell viability in cardiomyocytes and cardiac fibroblasts. STAT3 small interfering RNA (siSTAT3) was applied to knockdown STAT3 in cardiomyocytes and cardiac fibroblasts (Fig. 7a, b). SiSTAT3 treatment markedly repressed complexes I/II function, reduced cell viability and induced cell death in cardiomyocytes (Fig. 7c, e, g), whereas siSTAT3 treatment did not affect mitochondrial respiratory and cell survival of cardiac fibroblasts (Fig. 7d, f, g). These results indicated that STAT3 plays more an important role in mitochondrial respiratory function and cell protection in cardiomyocytes than in cardiac fibroblasts.

## Inhibition of STAT3 exacerbates $H_2O_2$-induced cell injury in cardiomyocytes but not obviously in cardiac fibroblasts

We further investigated the impact of STAT3 inhibition on $H_2O_2$-induced cell injury in both cardiomyocytes and cardiac fibroblasts. We also measured the mitochondrial complex function in cardiomyocytes and cardiac fibroblasts after $H_2O_2$ treatment (100 μM, 4 h) under STAT3 knockdown conditions. STAT3 knockdown using STAT3 siRNA exacerbated $H_2O_2$-induced impairment of mitochondrial function, $H_2O_2$-induced decrease of cell viability and cell survival in cardiomycytes (Fig. 8a, c, e). However, STAT3 knockdown showed no significant effect on mitochondrial function, cell viability and cell survival of cardiac fibroblasts which were under $H_2O_2$ treatment (Fig. 8b, d, e).

In addition to using siSTAT3, we further used STAT3 inhibitor S3I-201 to study the role of STAT3 in mitochondrial function and cell viability of cardiomyocytes and cardiac fibroblasts. S3I-201 treatment reduced the protein level of p-STAT3 (Y705) in both types of cells (Fig. 9a, b),

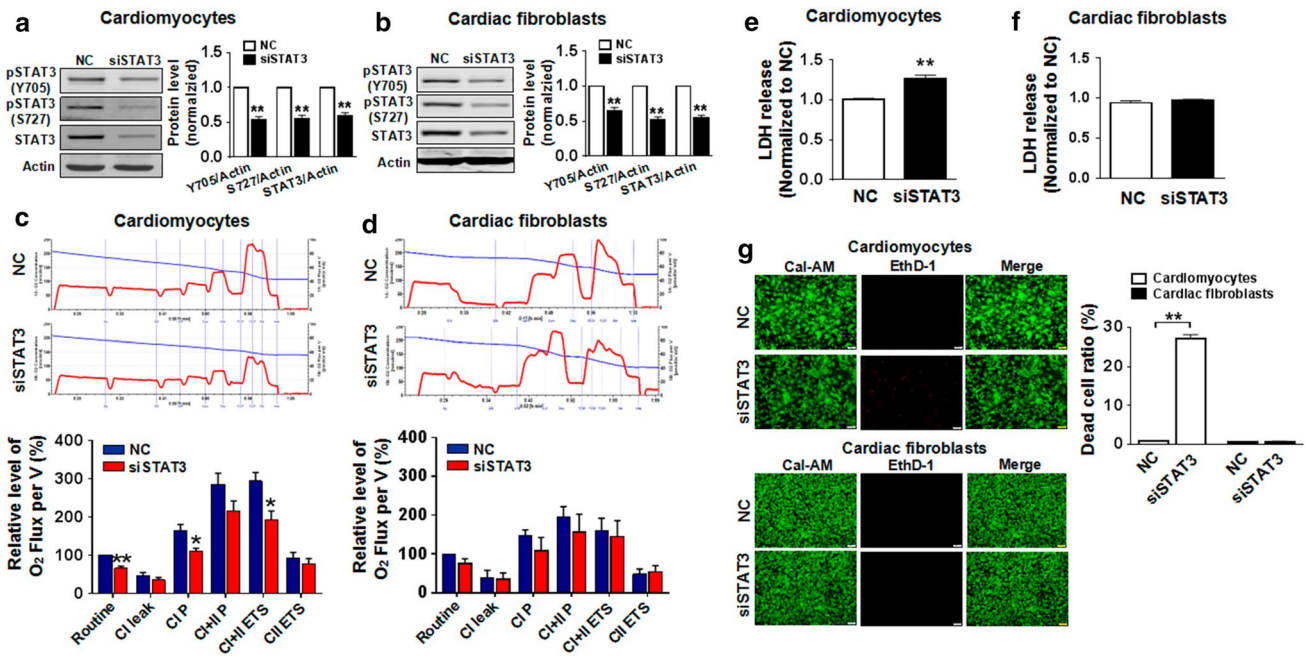


**Fig. 7** The effect of STAT3 knockdown using STAT3 siRNA (siSTAT3) on STAT3 protein expression, complex I/II-related mitochondrial respiratory function, and cell survival of cardiomyocytes and cardiac fibroblasts. **a**, **b** The verification of STAT3 knockdown using STAT3 siRNA in cardiomyocytes ($n=6$) and cardiac fibroblasts ($n=8$). $^{**}P<0.01$ vs NC. *NC* negative control. **c**, **d** STAT3 knockdown using siSTAT3 reduced complex I/II-related mitochondrial respiratory function in cardiomyocytes but not cardiac fibroblasts, $n=6$, $^{*}P<0.05$ vs NC. *NC* negative control. **e**, **f** LDH release of cardiomyocytes and cardiac fibroblasts with STAT3 knockdown, $n=12$. **g** Live/dead staining results showed that in STAT3 knockdown included cell death of cardiomyocytes but not cardiac fibroblasts, $n=8$ images in each group. $^{**}P<0.01$ vs NC. *NC* negative control. Forty-eight hours after transfection, the cardiomyocytes and cardiac fibroblasts were collected for mitochondrial respiration and cell viability detection

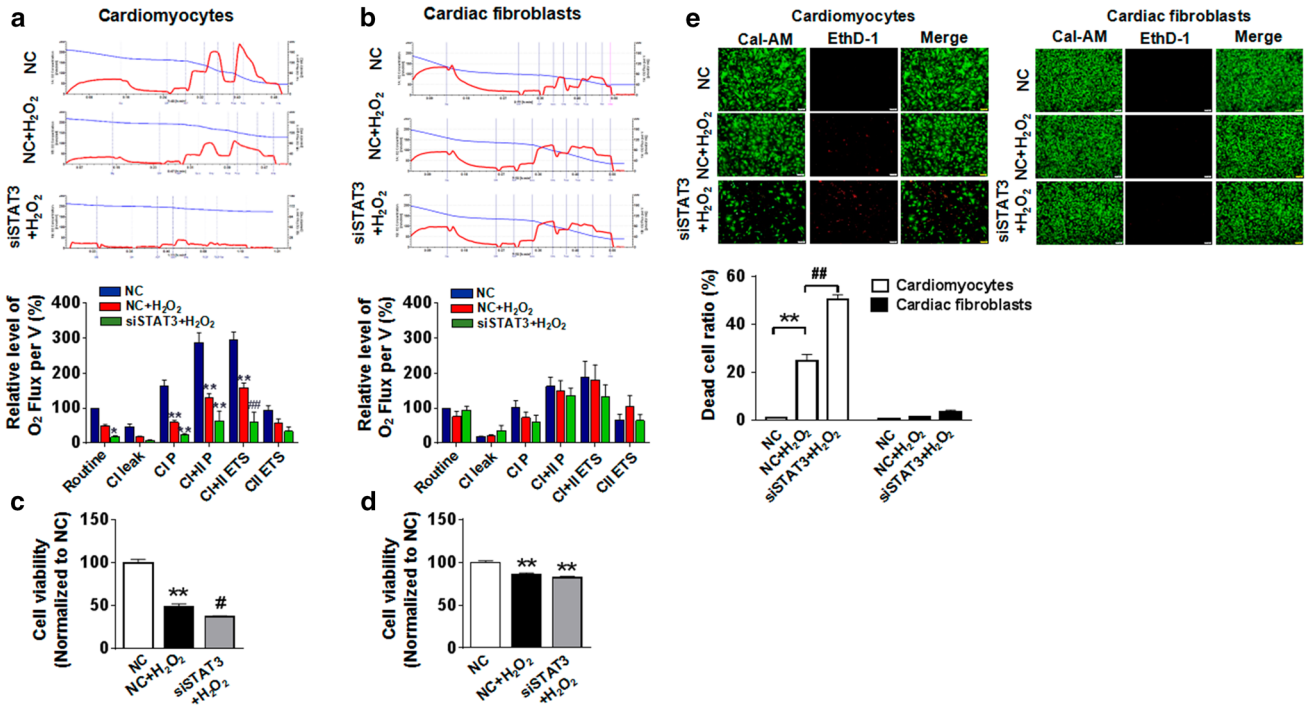


**Fig. 8** STAT3 knockdown exacerbates $H_2O_2$-induced impairment of mitochondrial respiration function and cell injury in cardiomyocytes but not cardiac fibroblasts. **a** The representative profiles and statistical data of mitochondrial respiration function of cardiomyocytes which were transfected with siSTAT3 or NC and treated with $H_2O_2$ (100 μM) for 4 h. $^{*}P<0.05$, $^{**}P<0.01$ vs NC. *NC* negative control, $n=6$. **b** The representative profiles and statistical data of mitochondrial respiration function of cardiac fibroblasts which were transfected with siSTAT3 or NC and treated with $H_2O_2$ (100 μM) for 4 h. *NC* negative control, $n=7$. **c** STAT3 knockdown exacerbated $H_2O_2$-induced reduction of cell viability in cardiomyocytes, $n=6$, $^{**}P<0.01$ vs NC, $^{\#}P<0.05$ vs NC + $H_2O_2$. **d** $H_2O_2$ (100 μM, 4 h) treatment slightly reduced cell viability of cardiac fibroblasts transfected with negative control, but STAT3 knockdown by siSTAT3 transfection did not exacerbate $H_2O_2$-induced reduction of cell viability, $n=6$. **e** Live/dead staining results showed that STAT3 knockdown exacerbated $H_2O_2$-induced cell death of cardiomyocytes but not cardiac fibroblasts, $n=8$ images in each group. $^{**}P<0.01$ vs NC, $^{\#\#}P<0.01$ vs NC + $H_2O_2$

indicating that S3I-201 could inhibit STAT3 activity. S3I-201 treatment alone showed no significant effect on cell viability of cardiomyocytes and cardiac fibroblasts, and only slightly inhibited CI + IIETS (CI plus CII electron transfer system) in cardiomyocytes (Fig. 9c–f).

However, under the $H_2O_2$ treatment (100 μM, 4 h) conditions, S3I-201 significantly exacerbated $H_2O_2$-induced impairment of mitochondrial respiratory function and cell injury in cardiomyocytes but not obviously in cardiac fibroblasts (Fig. 10), which is substantially consistent with the results of siSTAT3 treatment.

## Discussion

In this study, we have characterized the mitochondrial morphology and function of cardiomyocytes and cardiac fibroblasts, and found that the response of cardiomyocytes and cardiac fibroblasts to mitochondria inhibition was different. Under the $H_2O_2$ stimuli or rotenone treatment, mitochondrial function of cardiomyocytes was impaired and STAT3 signal was inhibited, which induced cardiomyocyte injury or increased susceptibility of cardiomyocytes to pathological stimuli; however, cardiac fibroblasts were not sensitive to these treatments, and whatever STAT3 inhibition or not, the cell viability or survival of cardiac fibroblasts was not significantly influenced by rotenone or $H_2O_2$ stimuli. Cardiomyocytes and cardiac fibroblasts are the dominant cell types of heart, and cardiomyocyte loss and cardiac fibrosis are the characterizations of major heart diseases, but the mechanism underlying the simultaneous occurrence of cardiomyocyte loss and cardiac fibroblast survival remains unclear. The present study provides novel understanding of the potential mechanism of cardiomyocyte loss and cardiac fibrosis under the same pathological stimuli. On the other hand, the present work also suggests that different signaling pathways might be in charge to transmit cellular stress in different cell types. STAT3 plays a critical role in the survival response in cardiomyocytes but not in cardiac fibroblasts which may have another alternative signal.

Cardiomyocytes constantly perform contractile function and need sustained energy supply. Cardiac fibroblasts

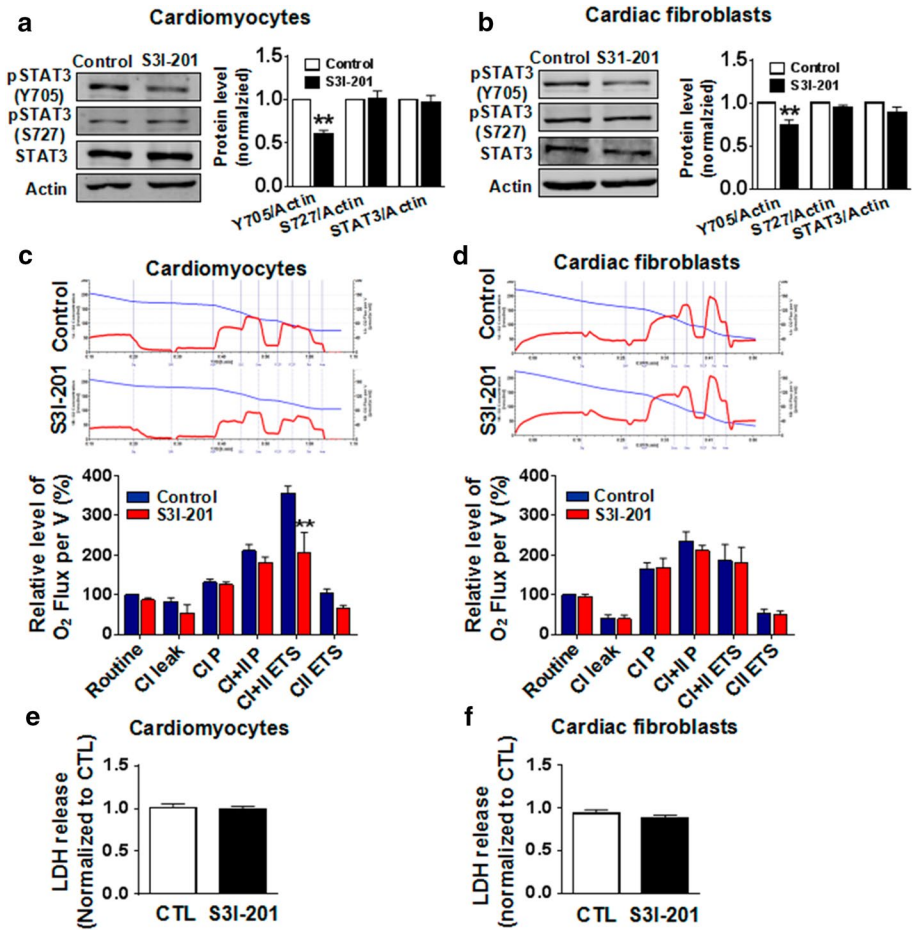


**Fig. 9** STAT3 inhibitor S3I-201 slightly inhibits complex I/II-related mitochondrial respiratory function in cardiomyocytes but not cardiac fibroblasts. **a** S3I-201 (10 μM) treatment for 12 h reduced the protein level of pSTAT3 (Y705) in cardiomyocytes, $n=6$. **b** S3I-201 (10 μM) treatment for 12 h reduced the protein level of pSTAT3 (Y705) in cardiac fibroblasts, $n=7$. **c** S3I-201 (10 μM) treatment for 12 h inhibited CI + IIETS (CI plus CII electron transfer system) in cardiomyocytes, $n=6$. **d** S3I-201 (10 μM) treatment for 12 h showed no effect on complex I/II-related mitochondrial respiratory function of cardiac fibroblasts, $n=6$. **e**, **f** S3I-201 (10 μM) treatment for 12 h showed no effect on LDH release in cardiomyocytes and cardiac fibroblasts, $n=6$, $^{**}P<0.01$ vs control (CTL)

are mainly responsible for synthesis and degradation of extracellular matrix to ensure proper cardiac form. Relatively to cardiomyocytes, cardiac fibroblasts may demand less energy. For adapting to their individual function, the mitochondria in cardiomyocytes and cardiac fibroblasts should have distinct distribution and density. Indeed, as shown in Fig. 1a, b of the mitochondrial staining, cardiomyocytes have high but cardiac fibroblasts have less mitochondrial density. The shape of mitochondria in cardiomyocytes and cardiac fibroblast was also distinct, the mitochondria of cardiomyocytes are mainly in spherical or ellipsoid shape and the mitochondria of cardiac fibroblasts are mainly in filamentous shape. We further compared the mitochondrial function and mitochondrial complex protein expression of cardiomyocytes and cardiac fibroblasts; results showed that the mitochondrial function and the complex I, II, III, IV, and V protein expressions of cardiac fibroblasts were significantly lower than those of cardiomyocytes. We speculate the reason that mitochondrial function of cardiac fibroblasts is lower than that of cardiomyocytes might be due to the difference of mitochondrial morphology, density, amount, and the expressions of mitochondrial complexes.

It has been reported that complex I/II activity was mainly diminished in severe heart diseases in vivo, for instance, Galan et al. found that myocardium after myocardial ischemia had reduced basal and maximal oxygen consumption rate, as well as complex I and II activity [8]; Schipper et al. reported that respiratory control rate and maximal complex I/II respiration ratio of mitochondrial isolates extracted from left atrial appendage tissue from patients were significantly lower [33]; Wüst et al. found that complex I/II-coupled respiration decreased in heart hypertrophy and heart failure of rats [42]. Therefore, we used complex I inhibitor rotenone as the tool to induce mitochondria inhibition because that its effect of inhibiting complex I activity was more close to pathological conditions in vivo. $H_2O_2$ is commonly used to induce myocardial injury [25, 40]; we used it as another model inducer. We established the experimental condition of 100 μM $H_2O_2$ for 4 h to treat cardiomyocytes and cardiac fibroblasts. This condition appropriately differentiated the response of the two types of cells to $H_2O_2$ stimulus, namely cardiomyocytes but not cardiac fibroblasts were damaged. Actually, $H_2O_2$ also induced injury of cardiac fibroblasts when the treatment time was prolonged or the concentration was increased (Supplementary Fig. 3). On

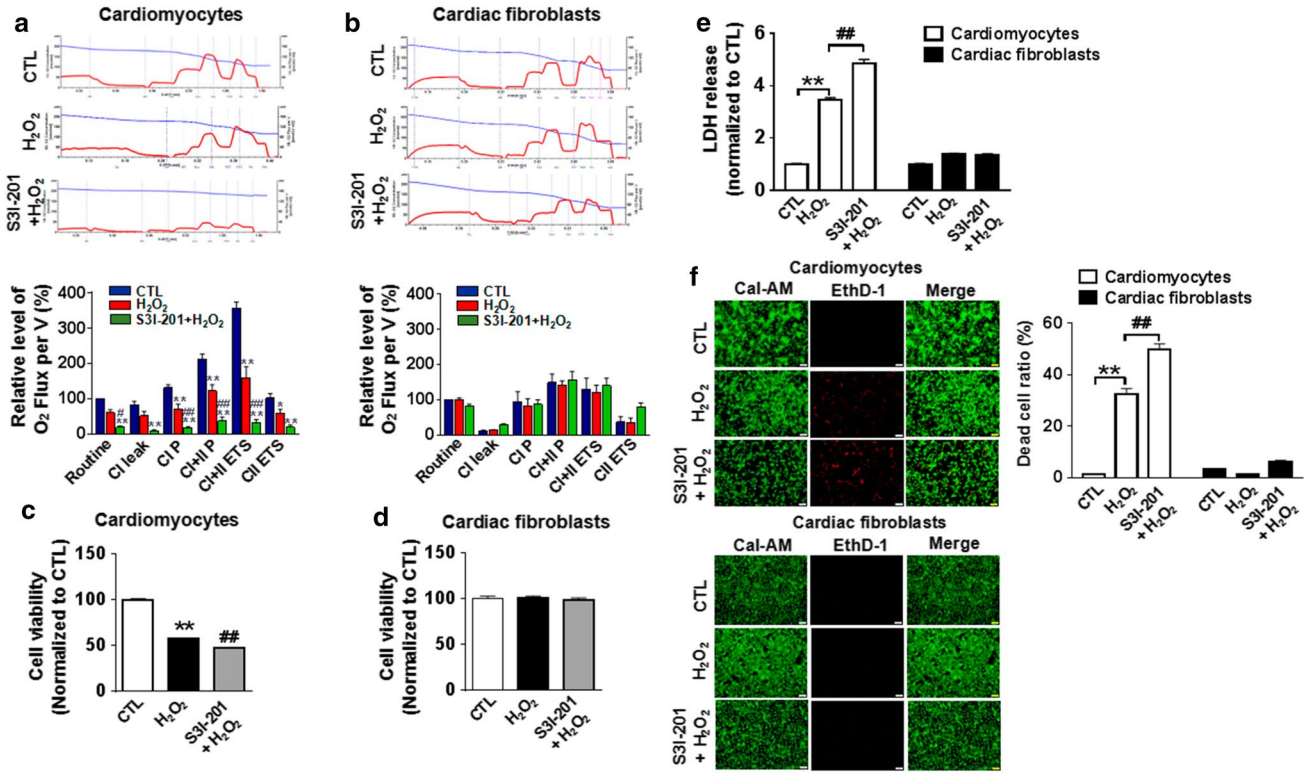


**Fig. 10** STAT3 inhibitor S3I-201 exacerbates $H_2O_2$-induced impairment of mitochondrial respiratory function and cell injury of cardiomycytes but not cardiac fibroblasts. **a** The representative profiles and statistical analysis of mitochondrial respiration in cardiomyocytes treated with $H_2O_2$ (100 μM) for 4 h combined pretreatment with or without S3I-201 (10 μM) for 12 h, $n=6$. **b** The representative profiles and statistics of mitochondrial respiration in cardiac fibroblasts treated with $H_2O_2$ (100 μM) for 4 h combined pretreatment with or without S3I-201 (10 μM) for 12 h, $n=6$. **c**, **d** The cell viability of cardiomyocytes and cardiac fibroblasts after $H_2O_2$ treatment (100 μM, 4 h) with or without pretreatment of S3I-201 (10 μM, 12 h), $n=6$. **e** LDH release in cardiomyocytes and cardiac fibroblasts after $H_2O_2$ treatment (100 μM, 4 h) with or without S3I-201 (10 μM,12 h), $n=6$. **f** The images and the statistics of live/dead staining of cardiomyocytes and cardiac fibroblasts stimulated with $H_2O_2$ (100 μM) combined with or without pretreatment of S3I-201(10 μM, 12 h). $n=10$, $^{*}P<0.05$, $^{**}P<0.01$ vs control, $^{\#}P<0.05$, $^{\#\#}P<0.01$ vs $H_2O_2$. *CTL* control

the whole, we concluded that mitochondria inhibition by rotenone and $H_2O_2$ stimulus showed different effect on the survival of cardiomyocytes and cardiac fibroblasts in the present experimental conditions, mitochondria inhibition induced damage of cardiomyocytes but had no effect on the survival and proliferation of cardiac fibroblasts.

STAT3 is a member of STAT family. STAT3 plays an important role in keeping cardiac physiological homeostasis and protecting the heart against injury [1, 11, 14, 16, 20]. The mechanism of STAT3-mediated cardioprotection is considered through two pathways: the canonical transcriptional action and the non-transcriptional regulation of electron transport chain (ETC). The canonical transcriptional action of STAT3 is that activated STAT3 translocates into the cell nucleus and activates a series of antiapoptotic and cardioprotective genes [2, 18]. The non-transcriptional regulation of ETC by STAT3 is that the mitochondria-localized STAT3 is required for optimal function of the ETC and reducing ROS production and cytochrome c release [38, 39, 41]. We found that knockdown of STAT3 by siRNA in cardiomyocyte reduced cell viability and induced cell death, and cardiomyocytes were more vulnerable to pathological stimuli when STAT3 was at inhibited state, confirming the protective role of STAT3 on cardiomyocytes.

Cardiac fibroblasts also express STAT3. In cardiac fibroblasts, STAT3 activation promoted cardiac fibroblast proliferation [13] and hyaluronan accumulation in the wound healing after acute myocardial infarction [27]. In heart tissue in situ, cardiomyocytes, endothelial cells, fibroblasts, as well as infiltrated immune cells co-exist and STAT3 is regarded as a key regulator of cell-to-cell communication [13]. Cardiomyocyte can stimulate STAT3 signal in cardiac fibroblasts through a paracrine mechanism [6]; it was reported that conditioned medium from STAT3-deficient cardiomyocytes increased fibroblast proliferation to promote fibrosis via paracrine factors [15]. In the present study, we found that mitochondria inhibition inhibited STAT3 in cardiomyocytes but not cardiac fibroblasts, so we speculated that cardiomyocytes with STAT3 inhibition by pathological stimuli might also promote fibrosis via paracrine mechanism in situ.

It was well known that STAT3 regulates mitochondrial respiration in cardiomyocytes [8, 46], but it is unclear whether mitochondrial function affects STAT3 signal in cardiomyocytes. In the present study, we found that both mitochondrial respiratory complex I inhibitor rotenone and $H_2O_2$ stimuli inhibited STAT3 in cardiomyocytes. Our previous study found that mitochondrial uncouplers induce biphasic change of mitochondrial function in parallel with the biphasic change of STAT3 activity in cardiomyocytes [10], indicating that mitochondrial function could regulate STAT3 signal in cardiomyocytes. However, in cardiac fibroblasts, inhibition of mitochondrial function showed no significant effect on STAT3 signal. We speculated that it might be due to that STAT3 signal in cardiac fibroblasts was not sensitive to mitochondrial function, or there existed a different mechanism of STAT3 regulation in cardiac fibroblasts from that in cardiomycytes.

In the present study, we used two ways to inhibit STAT3 signal, STAT3-siRNA (siSTAT3) and pharmacological inhibitor S3I-201. SiSTAT3 repressed both the expression and activity of STAT3 in cardiomyocytes and cardiac fibroblasts, and knockdown of STAT3 by siSTAT3 alone induced cardiomyocyte injury. S3I-201 only inhibited STAT3 activity [decreased protein level of p-STAT3 (Y705)] in cardiomyocytes and cardiac fibroblasts, and S3I-201 treatment alone showed no significant effect on cardiomyocytes and cardiac fibroblast. However, S3I-201 exacerbated $H_2O_2$-induced cell injury in cardiomyocytes but not in cardiac fibroblasts, which was consistent with the effect of siSTAT3. These results indicated that STAT3, whether in severe or slight inhibition state, could exacerbate pathological stimuli-induced cardiac injury. A previous study reported that STAT3-deficient mice showed enhanced susceptibility to myocardial ischemia with increased cardiac apoptosis and reduced survival [15]. A recent study reported that cardiac STAT3 expression decreased in peripartum cardiomyopathy patients and the low STAT3 expression sensitized to toxic effects of β-adrenergic receptor stimulation [35]. All these studies suggested the important role of STAT3 of cardiomyocytes against heart diseases.

The characterizations of neonatal and adult cardiac cells were different, for instance, the cell size, sarcomere components, and amount of mitochondria [9]. Considering differences between primary myocytes used in this study and adult myocytes, current data may not directly extrapolate to adult situation, which is a limitation. However, our findings first uncovered that STAT3 signaling is involved in the different susceptibility of cardiomyocytes and cardiac fibroblasts to mitochondrial inhibition, which contributed to distinct cardiac cell fate during pathologic conditions.

In conclusion, the present study mainly focused on the mitochondrial-dependent determination of cardiomyocytes and cardiac fibroblast cell fate during pathologic conditions. We demonstrated that the response of cardiomyocytes and cardiac fibroblasts to mitochondria inhibition was different. And STAT3 was uncovered as the key factor of different susceptibility of cardiac myocytes and cardiac fibroblasts to mitochondrial inhibition. Taken together, our study deepens our understanding of the pathological mechanism of severe heart diseases such as heart ischemia and heart failure, and provides novel potential approach for prevention or treatment of heart diseases.

**Funding** This work was supported by the National Natural Science Foundation of China (Nos. 81773725, 91739102).

## Compliance with ethical standards

**Conflict of interest** The authors declare that they have no conflict of interest.

## References

1. Boengler K, Ungefug E, Heusch G, Schulz R (2013) The STAT3 inhibitor stattic impairs cardiomyocyte mitochondrial function through increased reactive oxygen species formation. Curr Pharm Des 19:6890–6895
2. Bolli R, Stein AB, Guo Y, Wang OL, Rokosh G, Dawn B, Molkentin JD, Sanganalmath SK, Zhu Y, Xuan YT (2011) A murine model of inducible, cardiac-specific deletion of STAT3: its use to determine the role of STAT3 in the upregulation of cardioprotective proteins by ischemic preconditioning. J Mol Cell Cardiol 50:589–597. https://doi.org/10.1016/j.yjmcc.2011.01.002
3. Carbognin E, Betto RM, Soriano ME, Smith AG, Martello G (2016) Stat3 promotes mitochondrial transcription and oxidative respiration during maintenance and induction of naive pluripotency. EMBO J 35:618–634. https://doi.org/10.15252/embj.201592629
4. Coronado M, Fajardo G, Nguyen K, Zhao M, Kooiker K, Jung G, Hu DQ, Reddy S, Sandoval E, Stotland A, Gottlieb RA, Bernstein D (2018) Physiological mitochondrial fragmentation is a normal cardiac adaptation to increased energy demand. Circ Res 122:282–295. https://doi.org/10.1161/CIRCRESAHA.117.310725
5. Cui YC, Yan L, Pan CS, Hu BH, Chang X, Fan JY, Han JY (2018) The contribution of different components in QiShenYiQi Pills(R) to its potential to modulate energy metabolism in protection of ischemic myocardial injury. Front Physiol 9:389. https://doi.org/10.3389/fphys.2018.00389
6. Datta R, Bansal T, Rana S, Datta K, Datta Chaudhuri R, Chawla-Sarkar M, Sarkar S (2017) Myocyte-derived Hsp90 modulates collagen upregulation via biphasic activation of STAT-3 in fibroblasts during cardiac hypertrophy. Mol Cell Biol 37:e00611–e00616. https://doi.org/10.1128/MCB.00611-16
7. Dhingra R, Margulets V, Chowdhury SR, Thliveris J, Jassal D, Fernyhough P, Dorn GW 2nd, Kirshenbaum LA (2014) Bnip3 mediates doxorubicin-induced cardiac myocyte necrosis and mortality through changes in mitochondrial signaling. Proc Natl Acad Sci USA 111:E5537–E5544. https://doi.org/10.1073/pnas.1414665111
8. Galan DT, Bito V, Claus P, Holemans P, Abi-Char J, Nagaraju CK, Dries E, Vermeulen K, Ventura-Clapier R, Sipido KR, Driesen RB (2016) Reduced mitochondrial respiration in the ischemic as well as in the remote nonischemic region in postmyocardial infarction

remodeling. Am J Physiol Heart Circ Physiol 311:H1075–H1090. https://doi.org/10.1152/ajpheart.00945.2015
9. Galdos FX, Guo Y, Paige SL, VanDusen NJ, Wu SM, Pu WT (2017) Cardiac regeneration: lessons from development. Circ Res 120:941–959. https://doi.org/10.1161/CIRCRESAHA.116.309040
10. Gao JL, Zhao J, Zhu HB, Peng X, Zhu JX, Ma MH, Fu Y, Hu N, Tai Y, Xuan XC, Dong DL (2018) Characterizations of mitochondrial uncoupling induced by chemical mitochondrial uncouplers in cardiomyocytes. Free Radic Biol Med 124:288–298. https://doi.org/10.1016/j.freeradbiomed.2018.06.020
11. Gent S, Skyschally A, Kleinbongard P, Heusch G (2017) Ischemic preconditioning in pigs: a causal role for signal transducer and activator of transcription 3. Am J Physiol Heart Circ Physiol 312:H478–H484. https://doi.org/10.1152/ajpheart.00749.2016
12. Goldenthal MJ (2016) Mitochondrial involvement in myocyte death and heart failure. Heart Fail Rev 21:137–155. https://doi.org/10.1007/s10741-016-9531-1
13. Haghikia A, Ricke-Hoch M, Stapel B, Gorst I, Hilfiker-Kleiner D (2014) STAT3, a key regulator of cell-to-cell communication in the heart. Cardiovasc Res 102:281–289. https://doi.org/10.1093/cvr/cvu034
14. Heusch G, Musiolik J, Gedik N, Skyschally A (2011) Mitochondrial STAT3 activation and cardioprotection by ischemic postconditioning in pigs with regional myocardial ischemia/reperfusion. Circ Res 109:1302–1308. https://doi.org/10.1161/CIRCRESAHA.111.255604
15. Hilfiker-Kleiner D, Hilfiker A, Fuchs M, Kaminski K, Schaefer A, Schieffer B, Hillmer A, Schmiedl A, Ding Z, Podewski E, Podewski E, Poli V, Schneider MD, Schulz R, Park JK, Wollert KC, Drexler H (2004) Signal transducer and activator of transcription 3 is required for myocardial capillary growth, control of interstitial matrix deposition, and heart protection from ischemic injury. Circ Res 95:187–195. https://doi.org/10.1161/01.RES.0000134921.50377.61
16. Huang CH, Tsai MS, Chiang CY, Su YJ, Wang TD, Chang WT, Chen HW, Chen WJ (2015) Activation of mitochondrial STAT-3 and reduced mitochondria damage during hypothermia treatment for post-cardiac arrest myocardial dysfunction. Basic Res Cardiol 110:59. https://doi.org/10.1007/s00395-015-0516-3
17. Huang Z, Chen XJ, Qian C, Dong Q, Ding D, Wu QF, Li J, Wang HF, Li WH, Xie Q, Cheng X, Zhao N, Du YM, Liao YH (2016) Signal transducer and activator of transcription 3/MicroRNA-21 feedback loop contributes to atrial fibrillation by promoting atrial fibrosis in a rat sterile pericarditis model. Circ Arrhythm Electrophysiol 9:e003396. https://doi.org/10.1161/CIRCEP.115.003396
18. Kan J, Guo W, Huang C, Bao G, Zhu Y, Zhu YZ (2014) *S*-propargyl-cysteine, a novel water-soluble modulator of endogenous hydrogen sulfide, promotes angiogenesis through activation of signal transducer and activator of transcription 3. Antioxid Redox Signal 20:2303–2316. https://doi.org/10.1089/ars.2013.5449
19. Kanamori H, Takemura G, Goto K, Maruyama R, Ono K, Nagao K, Tsujimoto A, Ogino A, Takeyama T, Kawaguchi T, Watanabe T, Kawasaki M, Fujiwara T, Fujiwara H, Seishima M, Minatoguchi S (2011) Autophagy limits acute myocardial infarction induced by permanent coronary artery occlusion. Am J Physiol Heart Circ Physiol 300:H2261–H2271. https://doi.org/10.1152/ajpheart.01056.2010
20. Kleinbongard P, Skyschally A, Gent S, Pesch M, Heusch G (2017) STAT3 as a common signal of ischemic conditioning: a lesson on "rigor and reproducibility" in preclinical studies on cardioprotection. Basic Res Cardiol 113:3. https://doi.org/10.1007/s00395-017-0660-z
21. Lacraz GPA, Junker JP, Gladka MM, Molenaar B, Scholman KT, Vigil-Garcia M, Versteeg D, de Ruiter H, Vermunt MW, Creyghton MP, Huibers MMH, de Jonge N, van Oudenaarden A, van Rooij E (2017) Tomo-Seq identifies SOX9 as a key regulator of cardiac fibrosis during ischemic injury. Circulation 136:1396–1409. https://doi.org/10.1161/CIRCULATIONAHA.117.027832
22. Lew M (2007) Good statistical practice in pharmacology. Problem 2. Br J Pharmacol 152:299–303. https://doi.org/10.1038/sj.bjp.0707372
23. Liu H, Shao Y, Qin W, Runyan RB, Xu M, Ma Z, Borg TK, Markwald R, Gao BZ (2013) Myosin filament assembly onto myofibrils in live neonatal cardiomyocytes observed by TPEF-SHG microscopy. Cardiovasc Res 97:262–270. https://doi.org/10.1093/cvr/cvs328
24. Liu MY, Jin J, Li SL, Yan J, Zhen CL, Gao JL, Zhang YH, Zhang YQ, Shen X, Zhang LS, Wei YY, Zhao Y, Wang CG, Bai YL, Dong DL (2016) Mitochondrial fission of smooth muscle cells is involved in artery constriction. Hypertension 68:1245–1254. https://doi.org/10.1161/HYPERTENSIONAHA.116.07974
25. Matsuda T, Zhai P, Sciarretta S, Zhang Y, Jeong JI, Ikeda S, Park J, Hsu CP, Tian B, Pan D, Sadoshima J, Del Re DP (2016) NF2 activates hippo signaling and promotes ischemia/reperfusion injury in the heart. Circ Res 119:596–606. https://doi.org/10.1161/CIRCRESAHA.116.308586
26. Mukaddim RA, Rodgers A, Hacker TA, Heinmiller A, Varghese T (2018) Real-time in vivo photoacoustic imaging in the assessment of myocardial dynamics in murine model of myocardial ischemia. Ultrasound Med Biol 44:2155–2164. https://doi.org/10.1016/j.ultrasmedbio.2018.05.021
27. Müller J, Gorressen S, Grandoch M, Feldmann K, Kretschmer I, Lehr S, Ding Z, Schmitt JP, Schrader J, Garbers C, Heusch G, Kelm M, Scheller J, Fischer JW (2014) Interleukin-6-dependent phenotypic modulation of cardiac fibroblasts after acute myocardial infarction. Basic Res Cardiol 109:440. https://doi.org/10.1007/s00395-014-0440-y
28. Nguyen BY, Ruiz-Velasco A, Bui T, Collins L, Wang X, Liu W (2018) Mitochondrial function in the heart: the insight into mechanisms and therapeutic potentials. Br J Pharmacol. https://doi.org/10.1111/bph.14431
29. Nielsen SH, Mouton AJ, DeLeon-Pennell KY, Genovese F, Karsdal M, Lindsey ML (2017) Understanding cardiac extracellular matrix remodeling to develop biomarkers of myocardial infarction outcomes. Matrix Biol. https://doi.org/10.1016/j.matbio.2017.12.001
30. O'Sullivan KE, Breen EP, Gallagher HC, Buggy DJ, Hurley JP (2016) Understanding STAT3 signaling in cardiac ischemia. Basic Res Cardiol 111:27. https://doi.org/10.1007/s00395-016-0543-8
31. Paradies G, Petrosillo G, Pistolese M, Di Venosa N, Federici A, Ruggiero FM (2004) Decrease in mitochondrial complex I activity in ischemic/reperfused rat heart: involvement of reactive oxygen species and cardiolipin. Circ Res 94:53–59. https://doi.org/10.1161/01.RES.0000109416.56608.64
32. Pedrotty DM, Klinger RY, Kirkton RD, Bursac N (2009) Cardiac fibroblast paracrine factors alter impulse conduction and ion channel expression of neonatal rat cardiomyocytes. Cardiovasc Res 83:688–697. https://doi.org/10.1093/cvr/cvp164
33. Schipper DA, Palsma R, Marsh KM, O'Hare C, Dicken DS, Lick S, Kazui T, Johnson K, Smolenski RT, Duncker DJ, Khalpey Z (2017) Chronic myocardial ischemia leads to loss of maximal oxygen consumption and complex I dysfunction. Ann Thorac Surg 104:1298–1304. https://doi.org/10.1016/j.athoracsur.2017.03.004
34. Schirone L, Forte M, Palmerio S, Yee D, Nocella C, Angelini F, Pagano F, Schiavon S, Bordin A, Carrizzo A, Vecchione C, Valenti V, Chimenti I, De Falco E, Sciarretta S, Frati G (2017) A review of the molecular mechanisms underlying the development and progression of cardiac remodeling. Oxid Med Cell Longev 2017:3920195. https://doi.org/10.1155/2017/3920195
35. Stapel B, Kohlhaas M, Ricke-Hoch M, Haghikia A, Erschow S, Knuuti J, Silvola JM, Roivainen A, Saraste A, Nickel AG, Saar

JA, Sieve I, Pietzsch S, Muller M, Bogeski I, Kappl R, Jauhiainen M, Thackeray JT, Scherr M, Bengel FM, Hagl C, Tudorache I, Bauersachs J, Maack C, Hilfiker-Kleiner D (2017) Low STAT3 expression sensitizes to toxic effects of beta-adrenergic receptor stimulation in peripartum cardiomyopathy. Eur Heart J 38:349–361. https://doi.org/10.1093/eurheartj/ehw086

36. Su SA, Yang D, Wu Y, Xie Y, Zhu W, Cai Z, Shen J, Fu Z, Wang Y, Jia L, Wang Y, Wang JA, Xiang M (2017) EphrinB2 regulates cardiac fibrosis through modulating the interaction of Stat3 and TGF-beta/Smad3 signaling. Circ Res 121:617–627. https://doi.org/10.1161/CIRCRESAHA.117.311045
37. Sun B, Huo R, Sheng Y, Li Y, Xie X, Chen C, Liu HB, Li N, Li CB, Guo WT, Zhu JX, Yang BF, Dong DL (2013) Bone morphogenetic protein-4 mediates cardiac hypertrophy, apoptosis, and fibrosis in experimentally pathological cardiac hypertrophy. Hypertension 61:352–360. https://doi.org/10.1161/HYPERTENSIONAHA.111.00562
38. Szczepanek K, Chen Q, Larner AC, Lesnefsky EJ (2012) Cytoprotection by the modulation of mitochondrial electron transport chain: the emerging role of mitochondrial STAT3. Mitochondrion 12:180–189. https://doi.org/10.1016/j.mito.2011.08.011
39. Szczepanek K, Xu A, Hu Y, Thompson J, He J, Larner AC, Salloum FN, Chen Q, Lesnefsky EJ (2015) Cardioprotective function of mitochondrial-targeted and transcriptionally inactive STAT3 against ischemia and reperfusion injury. Basic Res Cardiol 110:53. https://doi.org/10.1007/s00395-015-0509-2
40. Wang JX, Zhang XJ, Li Q, Wang K, Wang Y, Jiao JQ, Feng C, Teng S, Zhou LY, Gong Y, Zhou ZX, Liu J, Wang JL, Li PF (2015) MicroRNA-103/107 regulate programmed necrosis and myocardial ischemia/reperfusion injury through targeting FADD. Circ Res 117:352–363. https://doi.org/10.1161/CIRCRESAHA.117.305781
41. Wegrzyn J, Potla R, Chwae YJ, Sepuri NB, Zhang Q, Koeck T, Derecka M, Szczepanek K, Szelag M, Gornicka A, Moh A, Moghaddas S, Chen Q, Bobbili S, Cichy J, Dulak J, Baker DP, Wolfman A, Stuehr D, Hassan MO, Fu XY, Avadhani N, Drake JI, Fawcett P, Lesnefsky EJ, Larner AC (2009) Function of mitochondrial Stat3 in cellular respiration. Science 323:793–797. https://doi.org/10.1126/science.1164551
42. Wust RC, de Vries HJ, Wintjes LT, Rodenburg RJ, Niessen HW, Stienen GJ (2016) Mitochondrial complex I dysfunction and altered NAD(P)H kinetics in rat myocardium in cardiac right ventricular hypertrophy and failure. Cardiovasc Res 111:362–372. https://doi.org/10.1093/cvr/cvw176
43. Xiao XL, Hu N, Zhang XZ, Jiang M, Chen C, Ma R, Ma ZG, Gao JL, Xuan XC, Sun ZJ, Dong DL (2018) Niclosamide inhibits vascular smooth muscle cell proliferation, migration, and attenuates neointimal hyperplasia in injured rat carotid arteries. Br J Pharmacol 175:1707–1718. https://doi.org/10.1111/bph.14182
44. Xie X, Zhao Y, Ma CY, Xu XM, Zhang YQ, Wang CG, Jin J, Shen X, Gao JL, Li N, Sun ZJ, Dong DL (2015) Dimethyl fumarate induces necroptosis in colon cancer cells through GSH depletion/ROS increase/MAPKs activation pathway. Br J Pharmacol 172:3929–3943. https://doi.org/10.1111/bph.13184
45. Xiong S, Wang P, Ma L, Gao P, Gong L, Li L, Li Q, Sun F, Zhou X, He H, Chen J, Yan Z, Liu D, Zhu Z (2016) Ameliorating endothelial mitochondrial dysfunction restores coronary function via transient receptor potential vanilloid 1-mediated protein kinase A/uncoupling protein 2 pathway. Hypertension 67:451–460. https://doi.org/10.1161/HYPERTENSIONAHA.115.06223
46. Zouein FA, Altara R, Chen Q, Lesnefsky EJ, Kurdi M, Booz GW (2015) Pivotal importance of STAT3 in protecting the heart from acute and chronic stress: new advancement and unresolved issues. Front Cardiovasc Med 2:36. https://doi.org/10.3389/fcvm.2015.00036